

A PROPOSED CAD MODEL BASED ON AMPLIFIED SPONTANEOUS EMISSION SPECTROSCOPY

F. V. Celebi*

Baskent University, Faculty of Engineering, Etimesgut 06530 Ankara-Turkey

Calculation of the optical quantities generally requires a large amount of computational time by using different theories, approximations and assumptions. In this study, a single, simple, new and an accurate computer aided design (CAD) model is successfully developed in strained quantum-well (QW) laser diodes in order to obtain the critical quantities and their dependences on wavelength and injection currents. These critical quantities are the modal gain difference, the induced refractive index difference, and the linewidth enhancement factor (Alpha parameter). The model is based on multilayer perceptron network (MLP) which is among the most important artificial neural network (ANN) architectures. Both the training and the test results are in very good agreement with previously designed InGaAsP strained QW laser diode results for long wavelength communication systems. The method is very useful for time saving purposes after finding the most suitable network configuration and can be easily used in the CAD design of optical communication systems.

(Received March 23, 2005; accepted May 26, 2005)

Keywords: Artificial neural Network, Laser diodes, Optical gain, Refractive index change, Linewidth enhancement factor, Optimisation

I. Introduction

While the applications of semiconductor laser diodes are continuously increasing in terms of complexity and sophistication, the CAD of these systems are vitally important for the prediction of the over all system response during the design phase. So many efforts are being made for the characterization of semiconductor materials as well as laser structures. One of these techniques named as amplified spontaneous emission (ASE) which has a long history of interest [1,2]. The ASE introduces noise through the system which degrades the system performance in optical communication systems. However the ASE spectrum of a semiconductor laser diode biased below threshold provides crucial information about some of the most important parameters which affect the performance of the whole system. These are the optical gain spectrum [3], refractive index change with injection current [4], and the linewidth enhancement factor [5].

In terms of the laser materials, one of the characteristic quantities is the optical gain which is undoubtedly among the most important parameters in semiconductor laser diodes. The optical gain contains significant information about the operating characteristics of the device and it is defined as the fractional increase in photons per unit length [6]. The optical gain at energy E is determined from spontaneous emission spectra [7]:

$$g = g_0 \left[1 - \exp\left(\frac{E - \Delta E_F}{kT}\right) \right] \quad (1)$$

where g_0 is a term related to spontaneous emission rate including the affect of thickness and number of wells, ΔE_F is the quasi-fermi level separation.

* Corresponding author: fatih@baskent.edu.tr

This is called the material gain, though it is the modal gain ($g_M = \Gamma g$, Γ is the optical confinement factor), which is obtained after some lengthy mathematical calculations. For an expanding rate of applications, an understanding of the gain spectra is very important in order to develop a model with predictive capability for the gain spectra of a certain diode laser structure. There are different methods proposed in literature to obtain the optical gain spectra [3] that provides different advantages and disadvantages in terms of the theoretical and experimental side. On the other hand, the improvements are still continuing in order to look for more accurate theoretical gain models and/or reliable gain measurement techniques.

The second quantity is the refractive index change with injection current which is required for the characterization of semiconductor laser diodes. It is closely related to the gain, and strongly affects the intra-cavity field distribution. The change in the refractive index is related to the gain spectrum through a Kramers-Kronig transformation. The induced change in the effective refractive index as a function of carrier density due to interband transitions can be written as [8]:

$$\delta n_e = \Gamma \frac{q^2 h^2}{m_0^2 L_z \epsilon_0} \sum_{n,m} \int \frac{k dk}{2\pi} |M_{nm}(k)|^2 \frac{[E_{nm}(k) - E]}{E_{nm}(k)[E_{nm}(k) + E]} \frac{[f_n^c(k) - f_m^v(k)]}{[E_{nm}(k) - E]^2 + \gamma^2} \quad (2)$$

where Γ is the optical confinement factor, L_z is the well width, m_0 is the electron resting mass, k is the crystal wave vector, M_{nm} is the momentum matrix elements between the n_{th} conduction band and m_{th} valance subbands, E_{nm} is the transition energy between the n_{th} conduction band and m_{th} valance subbands, f_n^c (f_m^v) is the Fermi occupation probability for electrons in the n_{th} (m_{th}) conduction (valance) subband, γ is the Lorentzian half-linewidth.

There are sophisticated theories of the carrier induced refractive index change in QW lasers for valance band mixing and nonparabolicity of the conduction bands [9], many particle effects [10], and taking in to account of all possible optical transitions [11]. Similar to optical gain spectra, the calculation of the refractive index change requires many calculations. In addition to that, the measurement of it is also difficult.

The last quantity is the linewidth enhancement factor (α parameter, LEF) which is one of the key parameters for semiconductor laser diodes under both high-speed direct modulation and CW operation. Since the spectral linewidth is proportional to $n_{sp}(1 + \alpha^2)$ where n_{sp} is the spontaneous emission rate, LEF has to be reduced in order to obtain a narrow spectral linewidth. A large value of LEF is detrimental since it increases the signal dispersion, mode chirping, and filamentation effects. On the other hand, high α parameter is useful in the generation of strongly chirped ultra-short optical pulses. It is the ratio of the derivatives with respect to carrier concentration of the real and imaginary parts of the complex dielectric function. In terms of the measurable quantities, it is proportional to the ratio of the changes in the refractive index and modal gain due to injection current, which is expressed as [12]:

$$\alpha = -\frac{4\pi}{\lambda} \frac{\frac{\partial n}{\partial N}}{\frac{\partial g_M}{\partial N}} \quad (3)$$

where $\partial g_M / \partial N$ is the differential gain and $\partial n / \partial N$ is the incremental change in the effective index due to carrier injection.

The calculation procedure of this parameter involves different approximations, assumptions and estimations which are pointed out in [13]. The difficulty is also known to measure the α parameter as it significantly varies with the operating wavelength, carrier density and other factors. The detailed estimation methods for α parameter are also given in [14].

Learning and generalisation ability, fast real-time operation and ease of implementation features make ANNs popular in recent years. ANNs are multipurpose computational methodologies with solid theoretical support and strong potential to be effective in any discipline. In these years, CAD approaches based on ANNs are introduced for optical quantities [13,15] for the purpose of modelling, simulation, and optimization. Therefore reliable, fast and accurate ANN models are developed in this way which can be used to speed up the optical designs. In this study, the theoretical and the experimental data [16] that are obtained from ASE spectroscopy for InGaAsP strained QW laser diode is used to develop a CAD model in order to find the modal gain difference, induced effective index difference, and the linewidth enhancement factor. The inputs of the CAD model are the wavelength and injection current respectively.

2. Development of the artificial neural network model

ANNs are new information-processing and computing technique inspired by biological neuron processing [17]. ANNs gather their knowledge by detecting the patterns and relationships in data and train through experience. An ANN is formed from many interconnected identical elements which are called artificial neurons or processing elements. These processing elements are connected each other with weights which constitute the ANN structure and are organised in layers. The power of ANN comes from the weight connection in a network. Each processing element has weighted inputs, summation function, activation function and output. The behaviour of an ANN is determined by the activation functions of its processing elements, by the learning rule, and by the architecture itself. The weights of the connections between the processing elements are adjusted during the training process to achieve the desired input/output of the network. During training, the connections between the units are optimised until the error in predictions is minimised and the network reaches the specified level of accuracy. When the training process is completed, the unused information is inputted to the network for the evaluation of the test results. ANN represents a promising modelling technique, especially for data sets having non-linear relationships that are frequently encountered in engineering. In terms of model specification, artificial neural networks require no knowledge of the data source but, since they often contain many weights that must be estimated, they require large training sets. In addition, ANNs can combine and incorporate both literature-based and experimental data to solve problems.

There are many types of ANN architectures [18] for various applications in the literature. Radial basis function networks and MLPs are the examples of feed forward networks which are capable of mimicking each other. MLPs [18] are the simplest and most commonly used ANN architectures which is shown in Fig. 1. In this paper, MLPs are used for the computation of modal gain difference, effective refractive index difference and the linewidth enhancement factor (alpha parameter) when the inputs are wavelength and injection current respectively. As shown in the figure, a MLP consists of three layers: an input layer, an output layer and one or more hidden layers with previously defined number of neurons. The neurons in the input layer only act as buffers for distributing the input signals x_i to neurons in the hidden layer. Each neuron j in the hidden layer sums up its input signals x_i , after weighting them with the strengths of the respective connections w_{ji} from the input layer and computes its output y_j as a function f of the sum, namely

$$y_j = f\left(\sum w_{ji} x_i\right) \quad (4)$$

where f is one of the activation functions used in ANN architectures.

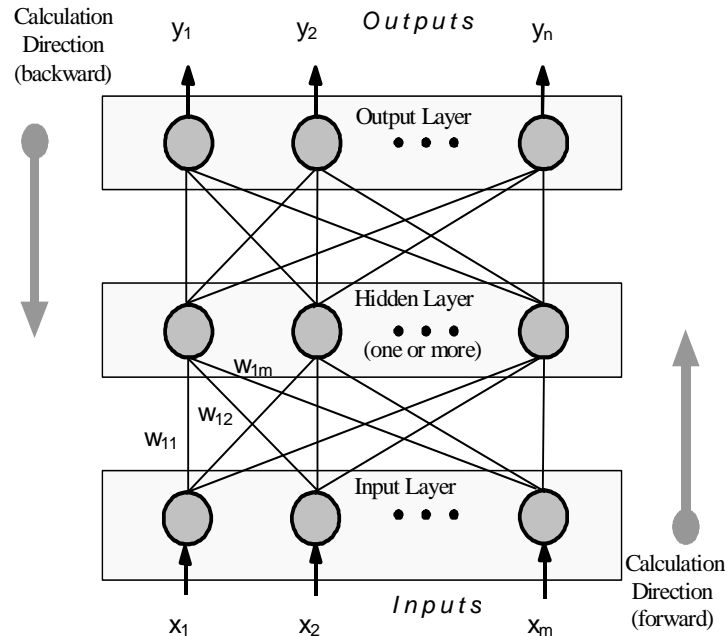


Fig. 1. General form of multilayer perceptrons.

The hidden layers allow modelling of complicated input/output relationships between multiple inputs and outputs by combining nonlinear activation functions. Inputs are connected to the first hidden layer by one set of weights and finally the last hidden layer is connected to the output layer by different set of weights. Training is completed successfully by optimising these weights to achieve the desired response with the use of a learning (optimisation) algorithm. A learning algorithm gives $\Delta w_{ji}(t)$ in the weight of a connection between neurons i and j at time t . The weights are then updated according to the following formula:

$$w_{ji}(t+1) = w_{ji}(t) + \Delta w_{ji}(t+1) \quad (5)$$

The proposed CAD modelling technique involves an ANN to calculate the output quantities modal gain difference; g_{MdANN} , effective refractive index difference; δn_{edANN} , and the linewidth enhancement factor; α_{ANN} (ANN outputs) when the injection current and wavelength values are given as inputs. Training the ANN with the use of different learning algorithms to calculate the g_{Md} , δn_{ed} , and α involves presenting it with different sets of input values and the corresponding measured values of g_{MdME} , δn_{edME} , and α_{ME} . Differences between the target outputs (g_{MdME} , δn_{edME} , α_{ME}) and the actual outputs of the ANN (g_{MdANN} , δn_{edANN} , α_{ANN}) are evaluated by the learning algorithms to adapt the weights using equations (4) and (5). There are many learning algorithms available in literature [18]. After several trials with different learning algorithms and with different network configurations in order to obtain a better performance with simpler structure, it is found that the most suitable network configuration is $2 \times 49 \times 5 \times 3$ with the Levenberg-Marquardt (LM) algorithm [19] which has a quadratic speed of convergence. This means that the number of neurons is 49 for the first hidden layer and 5 for the second hidden layer, respectively. The input and output layers have the linear activation function and the hidden layers have the hyperbolic tangent sigmoid activation function. The number of epoch is 300 for training. Before training, the input and the output data tuples are normalised between 0.0 and 1.0 in order to ensure the learning performance since the normalization is an essential step to improve the training process of ANNs.

After completing the training process successfully for all the critical optical quantities mentioned above in a single ANN model for injection currents 6 and 10 ma., test process is carried out for 8 ma. for the same critical quantities which is an indication of the generalization ability of the ANN model. The CAD model based on ANN in order to find the three critical quantities is shown in Fig. 2.

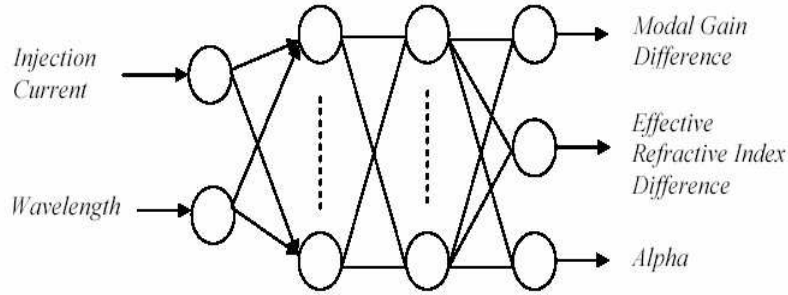


Fig. 2. Single ANN model for the computation of the critical quantities of InGaAsP strained QW laser diode.

The experimental data belongs to a buried heterostructure laser diode grown on an InP substrate which is designed for applications in long wavelength 1.55 μm . communication systems. The active region consists of five strained InGaAsP QWs with InGaAsP barriers. For other details of the device and the experimental values including experimental conditions, the reader can refer to [16].

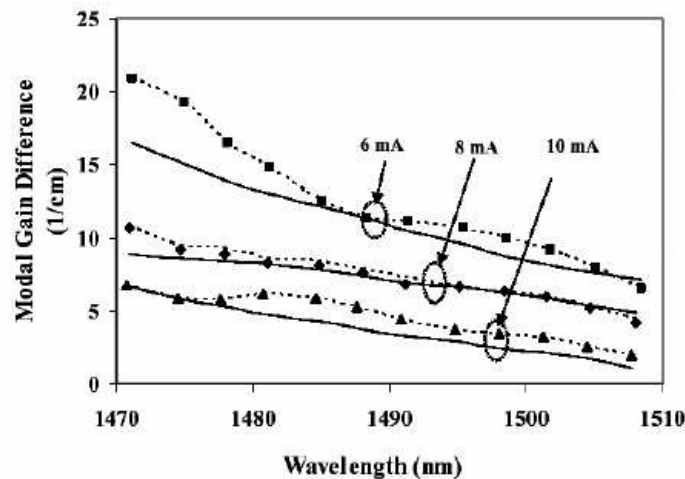
3. Results and conclusions

This study presents a new methodology for the CAD modelling of an optical device characteristics based on ANNs that can be used successfully and beneficially for the accurate determination of critical optical quantities. The developed ANN model is trained and tested with the LM learning algorithm which shows the best training and test results among other learning algorithms used in the analysis. In order to validate the accuracy of the model proposed in this paper, the ANN model results for g_{MdANN} , δn_{edANN} , and α_{ANN} are compared with the theoretical and experimental results (g_{MdME} , δn_{edME} , α_{ME}) reported in [16]. The mean square errors (mse) obtained from the CAD model is shown in table 1. It is clearly seen from the table that all of the optical quantities are in very good agreement with the measured values. In addition to that, the test mse errors between measured values and the model are much better than the mse errors between the measured values and the theoretical calculations. The results from the single proposed model support the validity of the CAD model even with the limited data set. The comparison of the results between measured, theoretical, and ANN model for each optical quantity for different injection currents are shown in Figs. 3, 4, and 5 respectively. The symbols are the experimental, solid curves are the theoretical, and dotted lines are the ANN results for each of these figures.

Table 1. The errors obtained from the single model for the whole optical quantities

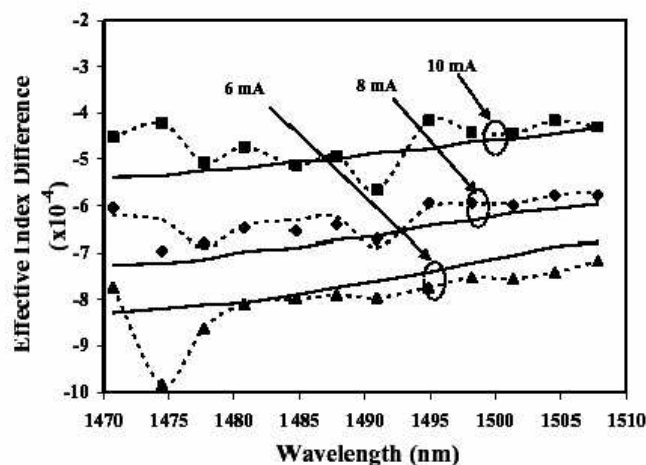
| OPTICAL QUANTITIES | MSE ERRORS | | |
|------------------------------------|----------------|------------------------------|---------------------------|
| | Training Error | Test Error (measured-theory) | Test Error (measured-ANN) |
| Modal Gain Difference | 3.07 exp (-31) | 0.361 | 0.063 |
| Effective Refrac. Index Difference | 1.07 exp (-30) | 0.220 | 0.047 |
| Alpha Parameter | 2.69 exp (-31) | 0.539 | 0.068 |

Even if the training time takes a few minutes after finding the most suitable configuration, the test process takes only a few microseconds to determine the values of the modal gain difference, effective refractive index difference, and the linewidth enhancement factor. It also needs to be clarified once more that better and more robust results can be obtained from ANN models if more data set values are supplied for training. The developed model demonstrates the versatility, robustness, and computational efficiency of the ANN based models. The classical calculation techniques require tremendous computational efforts by using complicated mathematics with the addition of and strong background knowledge. On the other hand, the proposed method is simple, inexpensive, very fast and accurate having very good agreement with the experimental results. It also does not require neither complicated mathematics nor strong background knowledge. At the same time It can be used for different engineering applications and purposes.



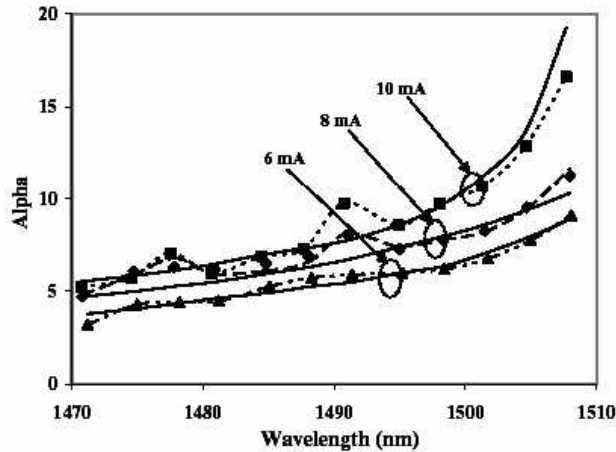
Symbols are experimental, solid curves are theoretical, dotted lines are ANN model results. 6 and 10 ma. current levels are the training results. 8 ma. is the test result.

Fig. 3. Comparison of the modal gain difference results obtained from ANN model, theory and measurements.



Symbols are experimental, solid curves are theoretical, dotted lines are ANN model results. 6 and 10 ma. current levels are the training results. 8 ma. is the test result.

Fig. 4. Comparison of the effective refractive index results obtained from ANN model, theory and measurements.



Symbols are experimental, solid curves are theoretical, dotted lines are ANN model results. 6 and 10 ma. current levels are the training results. 8 ma. is the test result.

Fig. 5. Comparison of the linewidth enhancement factor results obtained from ANN model, theory and measurements.

3. Conclusion

The proposed ANN model is capable of calculating the characteristic quantities of InGaAsP strained QW laser diode accurately under consideration. This kind of similar models can be developed for other optoelectronic devices, too, in order to be included in the CAD design of these systems.

References

- [1] L. Allen, G. I. Peters, *J. Phys. Pt A Gen* **4**(3), 377 (1971).
- [2] T. P. Lee, C. A. Burrus, B. I. Miller, *IEEE J. QE* **9**(8), 820 (1973).
- [3] W. H. Guo, Q. Y. Lu, Y. Z. Huang, L. J. Yu, *IEEE PTL* **15**(11), 1510 (2003).
- [4] A. Kimura, M. Nido, A. Suzuki, *IEEE PTL* **6**(9), 1101 (1994).
- [5] C. H. Henry, *IEEE J. QE* **18**(2), 259 (1982).
- [6] G. D. Sanders, C. K. Sun, J. G. Fujimoto, H. K. Choi, C. A. Wang, *Phys. Rev. B*, 8539 (1994).
- [7] G. Hunziker, W. Knop, P. Unger, C. Harder, *IEEE J. QE* **31**(4), 643 (1995).
- [8] S. L. Chuang, *Physics of Optoelectronic Devices*, Wiley, New York (1995).
- [9] M. S. Hybertsen, *Phys. Sim. IV*, **2994**, 747 (1997).
- [10] M. F. Pereira, S. W. Koch, W. W. Chow, *J. Opt. Soc. Amer. B, Opt. Phys.* **10**, 765 (1993).
- [11] H. Wenzel, G. Erbert, *IEEE J. ST QE* **5**, 637 (1999).
- [12] J. Hader, J. V. Moloney, S. W. Koch, *IEEE J. QE* **35**, 1878 (1999).
- [13] S. Sagiroglu, F. V. Celebi, K. Danisman, *Int. J. Electron. Comm. (AEU)* **56**(1), 51 (2002).
- [14] M. Osinski, J. Buus, *IEEE J. QE* **23**, 9 (1987).
- [15] F. V. Celebi, K. Danisman, *J. Opt. Las. Tech.* **37**, 281 (2005).
- [16] C. S. Chang, S. L. Chuang, J. R. Minch, W. W. Fang, Y. K. Chen, *IEEE J. ST QE* **1**(4), 1100 (1995).
- [17] S. Haykin, *Neural Networks: a Comprehensive Foundation*, Macmillan College Publishing Company, Boston (2000).
- [18] F. M. Ham, I. Kostanic, *Principles of Neurocomputing for Science and Engineering*, Mc-Graw Hill, Singapore (2002).
- [19] M. T. Hagan, M. Menhaj, *IEEE Neural N.* **5**(6), 989 (1994).